Free energy of hydrophobic hydration

Straatsma, T. P.; Berendsen, H. J. C.; Postma, J. P. M.

Published in:
Journal of Chemical Physics

DOI:
10.1063/1.451846

Free energy of hydrophobic hydration: A molecular dynamics study of noble gases in water

T. P. Straatsma, H. J. C. Berendsen, and J. P. M. Postma

Citation: The Journal of Chemical Physics **85**, 6720 (1986); doi: 10.1063/1.451846
View online: https://doi.org/10.1063/1.451846
View Table of Contents: http://aip.scitation.org/toc/jcp/85/11
Published by the American Institute of Physics

Free energy of hydrophobic hydration: A molecular dynamics study of noble gases in water

T. P. Straatsma, H. J. C. Berendsen, and J. P. M. Postma[a)]
Laboratory of Physical Chemistry, University of Groningen, Nijenborgh 16, 9747AG Groningen, The Netherlands

(Received 19 May 1986; accepted 19 August 1986)

The potential utility and limitations of two methods to determine free energy differences from molecular dynamics simulations (MD) are studied. The computation of the free energy of hydration of the inert gases serves as a simple but illustrative example. Good results are obtained for the inert gases from a perturbation treatment, using a reference ensemble obtained from a MD simulation of a cavity in water, if these atoms are comparable in size to the cavity and the calculated free energy differences are small. This limits the applicability of the perturbation treatment of a small number of cases. Larger free energy differences can be obtained with reasonable accuracy from MD simulations with continuously changing interaction parameters. This integration method is more generally applicable, but makes an additional simulation necessary.

I. INTRODUCTION

One of the most important properties in the study of solvent effects is the free energy of solvation or interaction, which determines solubilities, partition coefficients, association, dissociation, and binding constants, phase equilibria, and for transition states, reaction rates. It is the purpose of this paper to show how free energies of solvation can be derived by computational methods from intermolecular interactions. We limit ourselves to aqueous solvation of simple hydrophobic solutes, as the inert gases.

The solvation process is considered to consist of two steps, (i) the formation of a repulsive cavity of appropriate size, and (ii) the introduction of the solute into this cavity. This division is common to many theories of solvation, notably the reasonably successful scaled particle theory (SPT).[1] Originally the SPT was developed for hard sphere fluids, for which exact relations can be derived. The method has been extended to one- and two-dimensional systems,[2] mixtures of rigid spheres,[3] and real fluids as water[4] and aqueous solutions.[5–7] For real fluids SPT incorporates severe approximations, both in the use of the hard sphere analogy and the perturbation treatment when a solute particle is introduced into the cavity. There is no way in which SPT can be refined such that its parameters can be derived from intermolecular interaction potentials.

A powerful approach to understand solution thermodynamics on the basis of intermolecular interaction potentials is the use of simulation methods as Monte Carlo or molecular dynamics (MD). These methods generate a representative ensemble of molecular configurations. The computation of free energy of cavity formation in water by MD methods has been the subject of previous publications[8,9] and Gibbs free energies of cavity formation at 300 K for cavity radii up to 3.8 Å will be reported.[10] The subject of the present paper is a MD study of the introduction of solutes into appropriate cavities. In a detailed analysis we compare various approximations, ranging from first order perturbation to MD simulations in which a solute is slowly grown into a cavity and the free energy difference is computed from the reversible work carried out in the process. The approach of dividing the solvation into two steps separates the problems connected with the introduction of a particle in a MD ensemble from the second step where the solute-solvent interaction potential is changed. Analysis of this second step permits a thorough evaluation of the applicability of the methods described in this paper to determine the free energy differences between systems that differ by substitution of one or a few atoms. The hydration of noble gases was chosen for its simplicity and the insight it gives into the use of MD to compute free energies. The method, especially the slow growth of particles or slow change of interaction parameters in the course of a MD run, is generally applicable and can be used for many processes of chemical and biochemical interest.[11]

II. THEORY

A. Perturbation of statistical reference ensembles

Consider a representative statistical isothermal–isobaric ensemble. The Gibbs free energy for this ensemble is related to the isobaric partition function[12] Δ

$$G = -kT \ln \Delta, \tag{1}$$

where

$$\Delta = \left(\frac{1}{h^{3N} N!}\right) \iiint \exp[-(H_0 + pv)/kT]\, dv\, dp^N\, dq^N. \tag{2}$$

$H_0(p^N,q^N)$ is the unperturbed Hamiltonian of the system and v is the volume. For any other system differing in the Hamiltonian by a perturbation of the potential energy $H_p = H_0 + \Delta V$, the difference in free energy is

[a)] Present address: European Molecular Biology Laboratory, D-6900 Heidelberg.

 0021-9606/86/236720-08$02.10

$$\Delta G = G_p - G_0 = -kT \ln\left(\frac{\Delta_p}{\Delta_0}\right). \quad (3)$$

The free energy difference can thus be expressed as an average of a function of the potential energy difference, since from Eqs. (2) and (3)

$$\Delta G = -kT \ln\langle \exp(-\Delta V/kT)\rangle. \quad (4)$$

The averaging is over the unperturbed isobaric–isothermal reference ensemble. Expanding the logarithmic and exponential function in Eq. (4) up to the order in ΔV leads to a first order perturbation result:

$$\Delta G = \langle \Delta V \rangle. \quad (5)$$

The evaluation of $\langle \Delta V \rangle$, where $\Delta V = \Sigma_{si} V_{si}(r_{si})$ is composed of individual interactions of the solute s with the solvent particles i, follows from the knowledge of the radial distribution function $g_s(r)$ of the reference solute–solvent distances, $\langle \Delta V \rangle = \rho_0 \int 4\pi r^2 g_s(r) V_{si}(r) dr$.

The evaluation of $\langle \exp(-\Delta V/kT)\rangle$ requires a representative ensemble of configurations. Since the generation of $g_s(r)$ by simulation requires such an ensemble anyway, the first order treatment of Eq. (5) offers little computational gain, while the accuracy is vastly inferior compared to the nonlinear perturbation treatment of Eq. (4).

From the MD simulation of some reference system an ensemble is obtained that represents a limited configuration subspace only. Thus the sampling in Eq. (4) cannot be performed over the entire configuration space as is necessary for general application of this method. Practical application in MD simulations is therefore restricted to cases where the important configuration subspace is sampled, i.e., contained in the reference ensemble from the simulation. This restriction leads to at least two criteria that have to be considered when using this method in practical cases.

First the applicability depends on the occurrence in the reference ensemble of a sufficient number of configurations in that range where the perturbation Boltzmann factor is important. Secondly, the magnitude of ΔG should not be too large.

The first criterion implies that there should be enough configurations contributing to $\langle \exp(-\Delta V/kT)\rangle$. Since this contribution is determined by the perturbation solute–solvent interaction potential of the solute, comparison of $\exp[-V_{\text{pert}}(r)/kT]$ with the radial solute–oxygen distribution function in the reference enemble gives a reasonable impression of the fraction of contributing configurations in the reference ensemble.

The second consideration is the magnitude of the calculated ΔG. For large ΔG calculated, the applied potential cannot be considered a perturbation to the reference ensemble. The perturbation potential then differs too much from the reference potential used to generate the configurations in the reference ensemble. In our studies we used a maximum of $2kT$. If the free energy difference is too large, the perturbations can be reduced by using additional simulations at intermediate values of the interaction parameters. This has been applied in a study of the hydration of ethane and ethanol.[13]

The first criterion for successful application of the perturbation treatment mentioned above needs some further examination and will be illustrated here on the perturbation of cavity reference ensembles with noble gas interaction potentials. In Fig. 1 three possible situations are given. In Fig. 1(a) the radial cavity–oxygen distribution of a particular cavity enemble is compared to the perturbation potential

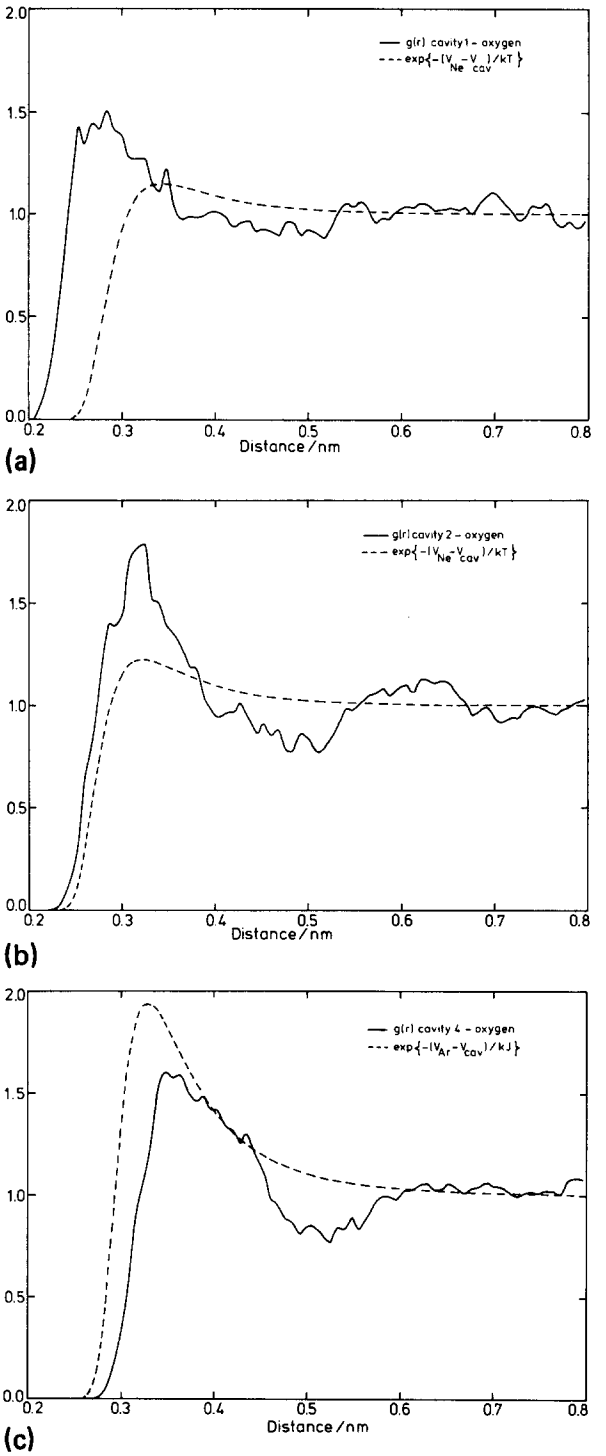

FIG. 1(a). Cavity–oxygen radial distribution function for reference ensemble of cavity 1. Dashed curve: free energy contribution $\exp(-V_{\text{pert}}/kT)$ for neon with this cavity ensemble; (b) Cavity–oxygen radial distribution function for reference ensemble of cavity 2. Dashed curve: free energy contribution $\exp(-V_{\text{pert}}/kT)$ for neon with this cavity ensemble; (c) Cavity–oxygen radial distribution function for reference ensemble of cavity 4. Dashed curve: free energy contribution $\exp(-V_{\text{pert}}/kT)$ for argon with this cavity ensemble.

function $\exp[-\Delta V_{\text{pert}}(r)/kT]$ for neon. Obviously most configurations have cavity–oxygen distances in a range where the perturbation does not significantly contribute to $\langle\exp(-\Delta V/kT)\rangle$. Since far too many configurations do not contribute, poor statistical information must be expected. In Fig. 1(c) a situation exists where the cavity chosen is too large. In the reference ensemble no configurations occur with cavity–oxygen distances in the range where $\exp[-V_{\text{pert}}(r)/kT]$ is important. Part of the contribution to the change in free energy is totally missing, and reliable results cannot be expected. A situation where the perturbation method is applicable is sketched in Fig. 1(b). From these arguments one must draw the conclusion that the best results can be expected from the perturbation method if the reference ensemble contains a cavity comparable in size or slightly smaller than the solute. For cavity reference ensembles this is a reformulation of the first criterion for practical application of the perturbation treatment, that can be interpreted in a more quantitative way.

B. The thermodynamic integration method

Instead of the computationally expensive method of using intermediate simulations, a continuous method can be used.[11] If the Hamiltonian is made a function of some parameter λ that changes from 0 to 1 in going from the initial system to the final system $H(\lambda) = H_0 + V(\lambda)$, with $V(0) = 0$ and $V(1) = V$, then the Gibbs free energy will be a function of λ also,

$$G(\lambda) = -kT \ln \Delta(\lambda), \tag{6}$$

where $\Delta(\lambda)$ is the isothermal–isobaric partition function,

$$\Delta(\lambda) = \left(\frac{1}{h^{3N}N!}\right)\iiint \exp\{-[H(\lambda) + pv]/kT\} \times dv\, dp^N\, dq^N. \tag{7}$$

Differentiating $G(\lambda)$ with respect to then leads to

$$\frac{\partial G(\lambda)}{\partial \lambda} = \left\langle \frac{\partial V}{\partial \lambda} \right\rangle_\lambda, \tag{8}$$

where the averaging is over the ensemble belonging to λ. As a special case V can be made a linear function of λ, $V(\lambda) = \lambda \Delta V$. The difference in Gibbs free energy between two systems for λ which is zero and unity can then be evaluated from integration of Eq. (8),

$$\Delta G = \int_0^1 \langle \Delta V \rangle_\lambda d\lambda. \tag{9}$$

The accuracy of ΔG calculated by Eq. (9) depends on the rate by which λ is increased from zero to unity during the simulation. It is essential that a particular configuration be statistically representative of the equilibrium distribution belonging to the Hamiltonian at λ. To obtain statistically meaningful configurations λ must increase gradually. In practice the rate by which λ should be increased will be determined by the potential energy difference between initial and final state and by the rate at which configurational relaxation takes place. If the final state differs radically from the initial state obviously this rate must be very low.

Some caution is needed when a potential term is added to the Hamiltonian representing the introduction of a particle into the system.[9] Special care must be taken then where to start this potential in phase space and what function must be chosen to increase λ since a drastic change is introduced. A simple linear growth of λ will not be satisfactory.

At every molecular dynamics step λ is changed and no equilibration at every λ is done. One therefore expects the configurations to lag behind the Hamiltonian used at λ. This results in a systematic error made every molecular dynamics time step. Since this is true also for a simulation backwards, $\lambda = 1 \rightarrow 0$, the hysteresis found provides a measure of the error due to not permitting the system to equilibrate at every step in λ.

III. COMPUTATIONAL DETAILS

A. The molecular dynamics simulations

All molecular dynamics simulations discussed in this paper were performed for an isothermal–isobaric ensemble of 216 water molecules with one solute in a box with periodic boundary conditions. Intermolecular interactions are taken into account within a cutoff radius of 0.9 nm. Intramolecular degrees of freedom are constrained using the SHAKE procedure.[14,15] All simulations extended over 40 ps using a time step of 1 fs. Weak coupling of the system to constant temperature (298 K) and pressure (1 bar) is applied with time constants of 0.4 and 0.5 ps for temperature and pressure. The algorithm is based on a leapfrog scheme with velocity and coordinate scaling at every dynamic step.[16]

B. Potentials

The potential model used for water in the molecular dynamics simulations is the simple point charge (SPC) model which is an effective pair potential derived from molecular dynamics simulations.[17] It consists of a negative charge of $-0.82\,e$ at the oxygen nucleus and two positive charges of $0.41\,e$ on tetrahedral positions at 0.1 nm from the oxygen. In addition the oxygens have a Lennard-Jones 6-12 interaction potential with parameters $\sigma = 0.317$ nm and $\epsilon/k = 78.2$ K, where σ is the collision diameter and ϵ/k the maximum depth of the potential well.

For the noble gas–water interactions Lennard-Jones 6–12 potentials were used for which parameters were obtained using the combination rules

$$\epsilon_{ws} = \sqrt{\epsilon_{ww} \cdot \epsilon_{ss}},$$
$$\sigma_{ws} = 0.5(\sigma_{ww} + \sigma_{ss}). \tag{10}$$

Neon parameters were taken from Geiger *et al.*[18] Parameters for the other noble gases were derived from values of Hirschfelder *et al.*[19] (see Table I).

The parameters for the potentials used are summarized in Table I. The cavity potentials consist of the repulsive part of a Lennard-Jones potential.

$$V_{\text{cav}} = 4\epsilon(\sigma/R)^{12}. \tag{11}$$

Ensembles of six cavity sizes were available from previous work. The size of a cavity is indicated by the thermal radius, defined as the value of $R = r_{\text{th}}$ for which $V_{\text{cav}}(R)$ equals kT.

TABLE I. Lennard-Jones parameters cavity- and solute-SPC oxygen.

Cavity	$4\epsilon\sigma^{12}$ kJ nm^{12} mol^{-1}	r_{th} nm	$\Delta G_c^{8,9}$ kJ mol^{-1}
Cavity 1	0.25765	0.239	9.6(0.5)
Cavity 2	0.29099	0.270	14.2(0.7)
Cavity 3	0.32356	0.300	19.8(0.9)
Cavity 4	0.34280	0.318	23.5(1.1)
Cavity 5	0.36524	0.338	28.2

Solutes	σ nm	ϵ/k K	r_{th} nm
He	0.290	21.72	0.250
Ne	0.310	38.10	0.276
Ar	0.329	98.87	0.307
Kr	0.342	114.97	0.321
Xe	0.357	129.60	0.336

C. Statistical errors from simulation calculations

The statistical errors were calculated using a method in which the correlation of the resulting series is used explicitly[20] rather than using the more commonly employed procedure of taking the variance of averages of subseries. Since an analysis of the correlation should be made anyway in order to justify a particular choice of the number of subseries it is far better to use all information provided by the correlation function.

The variance of the mean in the method used is given by

$$\mathrm{Var}(\bar{X}) = \frac{c_0}{n}\left[1 + 2\sum_{k=1}^{n-1}(1 - (k/n)\rho_k\right], \qquad (12)$$

where c_0 is $\mathrm{Var}(X_i)$ and ρ_k is the autocorrelation function as calculated from the data.

IV. THERMODYNAMICS OF HYDROPHOBIC HYDRATION

The process to be described is the solvation of hydrophobic solutes in water, at infinite dilution. The standard Gibbs free energy of transfer of 1 mol of a substance X from its ideal gas phase at standard pressure p° and temperature T to an ideal solution, in the sense of Henry's law, with standard mole fraction $x = 1$, at the same pressure and temperature, is given by[7]

$$\Delta G^\circ = \Delta G_c + \Delta G_i + RT\ln\frac{RT}{p^\circ v_m}, \qquad (13)$$

where v_m is the molar volume of the solvent (water). ΔG_c is the isobaric reversible work to create a cavity with a given radius and ΔG_i is the reversible work to introduce into this cavity the potential representing the solute. For the noble gases the internal partition function is the same in the gas phase and in solution. The Gibbs free energy ΔG° is related to Henry's constant K_H, the ratio between gas fugacity and the mole fraction in a saturated solution of the gas, that can be determined experimentally,

$$\Delta G^\circ = RT\ln K_H. \qquad (14)$$

TABLE II. Free energy of hydration from perturbation.

$\Delta G_i = RT\ln\langle\exp(-\Delta V/kT)\rangle$ kJ mol^{-1}

Perturbation potential	Reference ensemble: Cavity 2	Cavity 3	Cavity 4
Ne$\langle\Delta V\rangle$	− 2.6	− 9.7	− 10.9
Ne	− 3.6(0.3)	− 11.3(1.1)	− 13.8(0.7)
Ar	− 5.9(1.7)	− 13.5(0.6)	− 17.3(0.3)
Kr	− 5.6(1.6)	− 12.5(0.9)	− 17.6(0.4)
Xe	− 2.3(2.6)	− 12.3(1.2)	− 17.5(0.8)

$\Delta G^\circ = \Delta G_c + \Delta G_i + RT\ln\frac{RT}{p^0 v_m}$ kJ mol^{-1}

Perturbation potential	Reference ensemble: Cavity 2	Cavity 3	Cavity 4	Expt (Ref. 26)
Ne	10.7(1.0)	8.5(1.0)	9.6(1.8)	10.366
Ar	8.3(2.4)	7.3(1.5)	6.2(1.4)	8.3126
Kr	6.7(2.3)	7.5(1.8)	5.9(1.5)	6.956
Xe	11.9(3.3)	7.0(2.1)	6.0(1.9)	6.056

V. RESULTS

A. Neon

The best suitable cavity size to accommodate the neon potential ($r_{th} = 0.276$ nm) is the reference ensemble from cavity 2 ($r_{th} = 0.270$ nm). The change in Gibbs free energy for this perturbation is -3.6 ± 0.3 kJ mol^{-1}. The second condition to apply the perturbation method, $|G| < 2kT$, is thus also met. The calculated free energy of solution is 10.7 ± 1.0 kJ mol^{-1}. ΔG° can also be obtained from the reversed perturbation, using a molecular dynamics simulation of neon in water and perturbing the resulting ensemble with the cavity potential. The resulting value 10.7 ± 1.2 kJ mol^{-1} is also somewhat above the experimental value of 10.36 kJ mol^{-1}. Smaller perturbations are expected to give more accurate results. From a simulation of water with a solute–particle with a Lennard-Jones interaction potential $\frac{1}{2}(V_{cav} + V_{Ne})$ this free energy can be derived in two steps.

TABLE III. Free energy of hydration for neon from perturbation results.

Perturbation	Reference: Cavity 2	$\frac{1}{2}(V_{cav2} + V_{Ne})$	Neon
ΔG_i kJ mol^{-1}			
Cavity 2		2.02(0.05)	3.5(0.5)
$\frac{1}{2}(V_{cav2} + V_{Ne})$	− 1.6(0.2)		2.11(0.05)
Neon	− 3.6(0.3)	− 2.23(0.03)	
ΔG°(Ne)kJ mol^{-1}			
Cavity 2 → neon			10.7(1.0)
Cavity 2 → $\frac{1}{2}(V_{cav2} + V_{Ne})$ → neon			10.4(0.9)
Neon → cavity 2			10.7(1.2)
Neon → $\frac{1}{2}(V_{cav2} + V_{Ne})$ → cavity 2			10.1(0.8)
Experimental (Ref. 26)			10.36

TABLE IV. Free energy of hydration from MD growth results.

Inert gas	Path	Time ps	ΔG_i kJ mol^{-1}	$\Delta G°$ kJ mol^{-1}	Hysteresis kJ mol^{-1}	$G°_{exp}$ (Ref. 26) kJ mol^{-1}
Ne	cavity 2→Ne	40	−4.00	10.22		
	Ne→cavity 2	40	4.06	10.16		
				10.19	0.06	10.36
Xe	cavity 4→Xe	40	−23.1	5.1		
	Xe→cavity 4	40	23.5	4.7		
				4.9	0.4	6.1
Xe	neon→xenon	15	−2.56	7.6		
	xenon→neon	15	1.99	8.2		
				7.9	0.6	6.1

The values obtained, 10.4 kJ mol^{-1} and vice versa 10.1 kJ mol^{-1}, are within the statistical error in good agreement with the experimental value. Results for the perturbations are summarized in Tables II and III. Note that the first order perturbation $\Delta G = \langle \Delta V \rangle$ is too crude an approximation.

The Gibbs free energy of solution was also computed for neon using the continuous method of integration. In 40 ps the solute potential changed linearly in the molecular dynamics simulation, from cavity 1 to the neon potential and vice versa. ΔG_i calculated from both simulations is −4.0 and −4.1 kJ mol^{-1}. The hysteresis is about 0.1 kJ mol^{-1} and can be regarded as a measure of the accuracy with which $\Delta G°$ with this method can be calculated. $\Delta G°$ in the these two cases is 9.9 ± 0.8 and 10.1 ± 0.8 kJ mol^{-1}. Considering the statistical uncertainty again good agreement with experiment is found. Results for the thermodynamic integration are given in Table IV. The change in free energy is depicted in Fig. 2.

Note that the major part of the statistical error stems from the ΔG_c for creating a cavity in water 0.7 kJ mol^{-1}, due to the accumulation of this error with the connection of adjacent simulations for several cavity sizes. An overview of the results for neon is given in Fig. 3. Errors are given for the perturbation contributions ΔG_i. All calculated values are within statistical error in excellent agreement with experiment.

B. Argon

The best cavity simulation on which the argon potential can be taken as a perturbation would be cavity 3

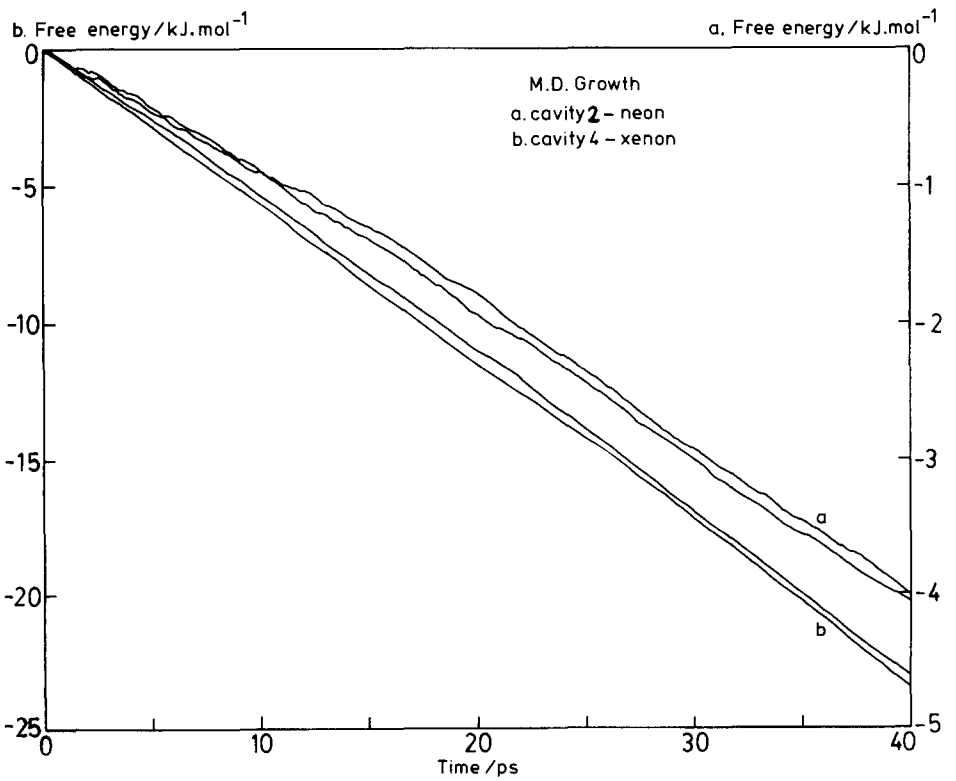

FIG. 2. Free energy change growing (a) neon into cavity 2 in 40 ps (right-hand side axis); (b) xenon into cavity 4 in 40 ps (left-hand side axis).

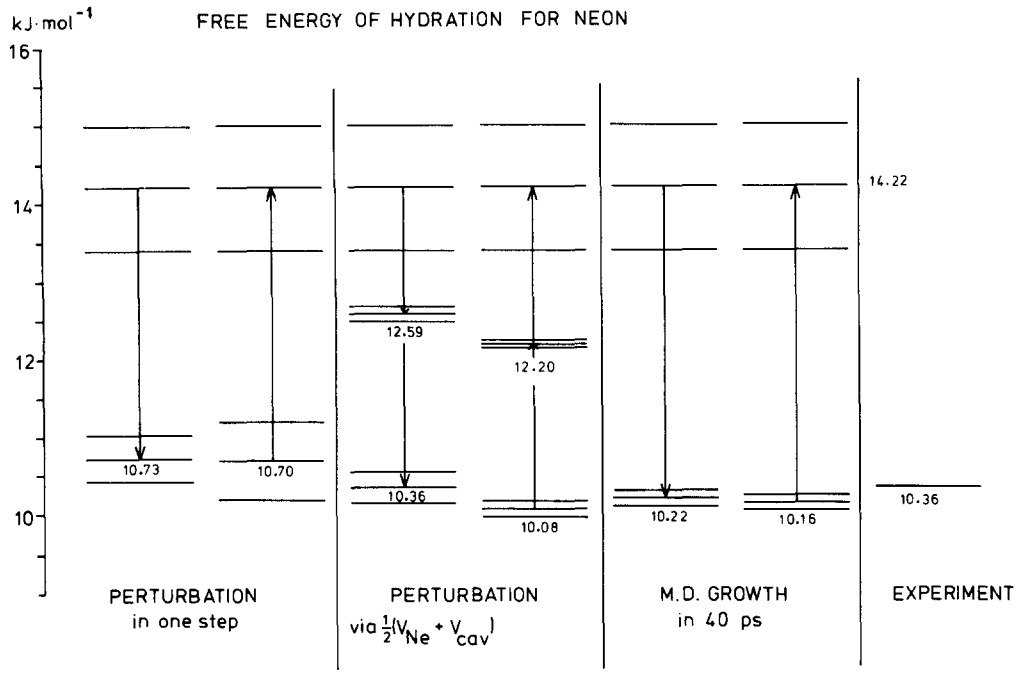

FIG. 3. Free energy of hydration for neon by perturbation method and MD growth. Statistical errors are given by the extra lines above and below the indicated levels. The levels at 14.22 kJ mol^{-1} refers to the cavity used as a reference indicated with its own accuracy. Statistical errors for the other levels refer to the change in free energy with respect to the cavity.

($r_{th} = 0.300$ nm), according to the argon size (0.307 nm). The calculated $\Delta G_i = -13.5 \pm 0.6$ kJ mol^{-1} however does not match the second condition to use the perturbation method. Argon cannot be regarded as a small perturbation to this cavity. As pointed out in Sec. II A a simulation of a smaller cavity may be used as a reference ensemble at the expense of statistical accuracy. Using the cavity 2 reference ensemble, $\Delta G_i = -5.9$ kJ mol^{-1} is calculated. Now ΔG_i is comparable to $2kT$ and the Gibbs free energy of solution of argon in water is $\Delta G^\circ = 8.3 \pm 2.4$ kJ mol^{-1}. This value is exactly the experimental value, but as expected the statistical error is large (see Table II).

C. Krypton

For krypton a discussion similar to the argon perturbation may be held. The best cavity size to accommodate krypton would be cavity 4. However the calculated ΔG_i is far too high to justify the krypton potential as a perturbation to this cavity. When ΔG_i is calculated using again the reference ensemble of cavity 2, then -5.6 ± 1.6 kJ mol^{-1} is found resulting in $\Delta G^\circ = 6.7 \pm 2.3$ kJ mol^{-1}. In spite of the large statistical error this value is surprisingly close to the experimental value of 6.95 kJ mol^{-1}.

D. Xenon

In the xenon case the cavity ensemble that gives an acceptable ΔG_i to use the perturbation methods leads to a statistical error larger than the ΔG_i itself. Secondly in this case this cavity is certainly far too small to accommodate xenon. The only option left to compute ΔG° for xenon is the use of intermediate simulations or the continuous method of integration.

Starting with an equilibrated configuration for cavity 4 xenon was grown linearly in 40 ps into the cavity and vice versa. ΔG_i calculated in these simulations are -23.1 and -23.5 kJ mol^{-1}. In Fig. 2 the ΔG_i change is shown as a function of time during the simulation. ΔG_i changes linearly and a small hysteresis is found of 0.4 kJ mol^{-1}. ΔG° calculated from these values is 5.1 and 4.7 kJ mol^{-1} respectively, about 1 kJ mol^{-1} less than the experimental value of 6.1 kJ mol^{-1}. Results are summarized in Table IV.

A particularly interesting situation arises when xenon is grown linearly from a neon configuration. The change in ΔG_i for a growth simulation from neon to xenon in 15 ps and vice versa is shown in Fig. 4. The sudden increase in ΔG_i starting at neon suggests that the surrounding water structure is distorted rather quickly in the first 2 ps. After 6 ps the surrounding water settles into a more favorable configuration to accommodate the xenon atom. This effect and the fact that the simulations were done in only 15 ps account for the large hysteresis of 0.6 kJ mol^{-1} as compared to the ΔG_i itself of -2.6 and 2.0 kJ mol^{-1}.

VI. DISCUSSION

The scaled particle theory is based on a statistical mechanical theory concerned with particles having spherical symmetry and hard cores. Although extensions have been made through the introduction of experimental densities and consideration of the attractive part of the intermolecular potential of a real liquid, application of the scaled particle theory remains limited. Reasonable accuracy cannot be expected for solvents having strong directional interactions, as in water, and for soft and nonspherical solutes.[21,22] The molecular dynamics method does not have these limitations and can be used to calculate free energy differences between similar more complex systems. In such cases the scaled particle theory will not be applicable at all.

In our treatment the polarization of the solute has not been taken into account. The calculated free energies should therefore be corrected, leading to somewhat lower values. The corrections are expected to be small, but not negligible for the heavier rare gases. The polarization energy $-\frac{1}{2}\alpha E^2$,

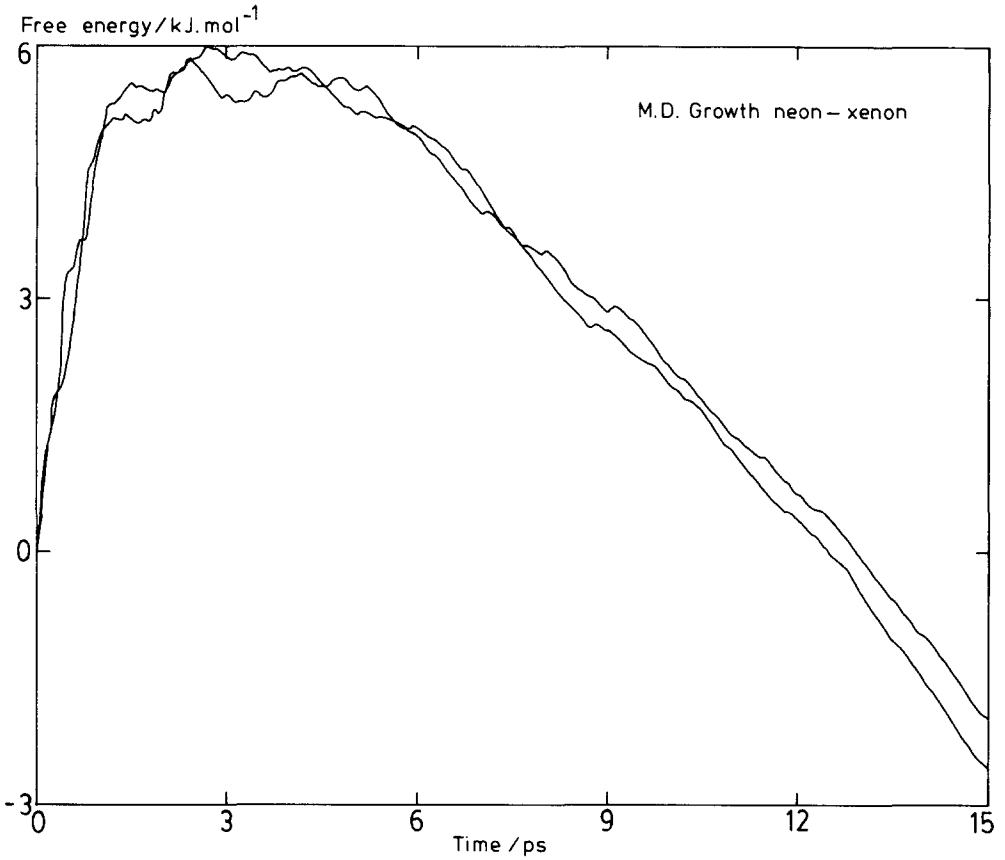

FIG. 4. Free energy change growing xenon from neon in 15 ps and v.v.

where E is the electric field at the center of the atom and α the atomic polarizability, for neon is 0.22 kJ mol^{-1} and for xenon[20] 0.98 kJ mol^{-1}. The polarization energies were determined as a first order perturbation on the configurations of the simulation in which polarizability was not taken into account. Experimental atomic polarizabilities have been used of 0.3946 and 4.04 Å^3, respectively.[23]

Provided a simulation of a reference ensemble is available, the perturbation method is an inexpensive method to obtain free energy differences. For the inert gases studied here surprisingly good results are obtained, when the two criteria mentioned in Sec. II A are considered. Perturbation theories always give more reliable results for smaller perturbations. The choice of $2kT$ as a limit to ΔG in the second criterion is therefore somewhat arbitrary. Increasing this value will increase the number of cases where perturbation theory can be used, but will also decrease the accuracy and reliability of the results obtained. From our studies $2kT$ seems a reasonable choice.

The integration method is not restricted to small changes in the Hamiltonian. For neon excellent agreement with experiment is found. For xenon grown from a cavity the change in free energy is much larger than for neon during the same simulation time. Consequently the hysteresis found is larger. The deviation of the resulting free energy of hydration from the experimental value is also larger. The behavior of the free energy change with time in these cases is similar, and linear, as can be seen from Fig. 2. The accuracy of this method is thus, as expected, dependent on the magnitude of the total free energy change. Two drastically differing systems will need a large simulation time span in this method to find the free energy difference with sufficient accuracy. The free energy change per time step also has to be considered, as is illustrated by the simulation in which neon is gradually changed into xenon in 15 ps. The total free energy difference is smaller, but the change per time step is much large than in the former two cases. Although the accuracy could be improved by a longer simulation, this will not change the path followed by the Hamiltonian that is responsible for the behavior of the ΔG_i curve during the simulation. The choice of a different path along which the solute–solvent potential is changed from initial to final state can overcome the large changes in conformation in the course of the simulation. In our application we have used λ as a linear scaling parameter for the complete solute–solvent potential. An elegant alternative is to make σ and ϵ separately dependent on λ, as proposed by Cross.[24]

If the behavior of ΔG_i is nonlinear but monotonous it is better to make λ a nonlinear function of time. Thus the path will not change, but with a sensible choice of this function one may hope to vary the change in the Hamiltonian in such a way that the free energy $\Delta G_i(t)$ changes linearly with time. It is obvious that the change in free energy should be carefully monitored during the simulation in order to be able to discuss the accuracy obtained.

Results from both the perturbation method and the integration method depend strongly on the solute–solvent potentials. Since rather simple model potentials are used, one has to be careful in comparing results obtained with these methods with experimental values. On the other hand free energy evaluations can be important to judge the validity of realistic model potentials.

The results presented in this paper, together with other perturbation results,[13,25] indicate the power and potential applicability of the methods used, also for more complex systems. Especially in biological systems where small changes may lead to important differences in chemical behavior the outlined methods may prove to be of great importance.[11]

ACKNOWLEDGMENT

This research was supported by the Foundation for Chemical Research (SON) under the auspices of the Netherlands Organization for the Advancement of Pure Research (ZWO).

[1]H. Reiss, H. L. Frisch, and J. L. Lebowitz, J. Chem. Phys. **31**, 369 (1959).
[2]E. Helfand, H. L. Frisch, and J. L. Lebowitz, J. Chem. Phys. **34**, 1037 (1961).
[3]J. L. Lebowitz, E. Helfand, and E. Praestgaard, J. Chem. Phys. **43**, 774 (1965).
[4]F. H. Stillinger, J. Solution Chem. **2**, 141 (1973).
[5]R. A. Pierotti, J. Chem. Phys. **67**, 1840 (1963).
[6]R. A. Pierotti, J. Chem. Phys. **69**, 281 (1965).
[7]R. A. Pierotti, Chem. Rev. **76**, 717 (1976).
[8]J. P. M. Postma, H. J. C. Berendsen, and J. R. Haak, Faraday Symp. Chem. Soc. **17**, 55 (1982).
[9]J. P. M. Postma, Thesis, Groningen, 1985.
[10]J. P. M. Postma, H. J. C. Berendsen, and W. F. van Gunsteren (unpublished).
[11]H. J. C. Berendsen, J. P. M. Postma, and W. F. van Gunsteren, in *Molecular Dynamics and Protein Structure*, edited by J. Hermans (Polycrystal Bookservice, Illinois, 1985), p. 43.
[12]D. A. McQuarrie, *Statistical Mechanics* (Harper and Row, New York, 1976).
[13]W. L. Jorgensen and C. Ravimohan, J. Chem. Phys. **83**, 3050 (1985).
[14]J. P. Ryckaert, G. Cicotti, and H. J. C. Berendsen, J. Comput. Phys. **23**, 327 (1977).
[15]W. F. van Gunsteren and H. J. C. Berendsen, Mol. Phys. **34**, 1311 (1977).
[16]H. J. C. Berendsen, J. P. M. Postma, W. F. van Gunsteren, A. DiNola, and J. R. Haak, J. Chem. Phys. **81**, 3684 (1984).
[17]H. J. C. Berendsen, J. P. M. Postma, W. F. van Gunsteren, and J. Hermans, in *Intramolecular Forces*, edited by B. Pullmann (Reidel, Dordrecht, 1981), p. 331.
[18]A. Geiger, A. Rahman, and F. H. Stillinger, J. Chem. Phys. **70**, 263 (1979).
[19]J. O. Hirschfelder, C. F. Curtiss, and R. B. Bird, in *Molecular Theory of Gases and Liquids* (Wiley, New York, 1954).
[20]T. P. Straatsma, H. J. C. Berendsen, and A. J. Stam, Mol.Phys. **57**, 89 (1986).
[21]M. Lucas, J. Chem. Phys. **80**, 359 (1976).
[22]N. M. Desrosiers and J. -P. Morel, Can. J. Chem. **59**, 1 (1981).
[23]C. G. Gray and K. E. Gubbins, in *Theory of Molecular Fluids* (Clarendon, Oxford, 1984), Vol. I.
[24]A. Cross (private communication).
[25]T. P. Lybrand, I. Ghosh, and J. A. McCammon, J. Am. Chem. Soc. **107**, 7793 (1985).
[26]F. Franks and D. S. Reid, in *Water, A Comprehensive Treatise*, edited by F. Franks (Plenum, New York, 1973), Vol. II.